

Technical note: Excess alkalinity in carbonate system reference materials

Jonathan D. Sharp, Robert H. Byrne *

College of Marine Science, University of South Florida, 140 7th Avenue South, St. Petersburg, FL 33701, USA

ARTICLE INFO

Keywords:

Certified reference materials
Organic alkalinity
Boron
CO₂ system

ABSTRACT

Certified reference materials (CRMs) for oceanic carbonate system measurements are critical for verifying the accuracy of laboratory protocols and the reliability of field sensors. CRMs are certified for total alkalinity and dissolved inorganic carbon, parameters that are (1) stable for a long period of time when a sample is properly stored and (2) not affected by changes in temperature and pressure. In experimentation initially designed to measure the total boron to salinity ratio of seawater, an interesting result has emerged regarding CRMs. A unique acidimetric titration method has indicated that three different batches of CRM contain excess alkalinity (i.e., alkalinity that is not attributable to inorganic bases included in the traditional definition of seawater total alkalinity) that is statistically greater than the excess alkalinity measured in open-ocean water from the Gulf of Mexico. Further, the amount of excess alkalinity appears to differ in certain CRM batches. Excess alkalinity in CRMs is likely caused by organic proton acceptors that are not completely oxidized by the ultraviolet sterilization procedure that CRMs undergo. The primary use of CRMs — to maintain the accuracy and consistency of carbonate system measurements — may be inhibited by excess alkalinity, which can cause differences in total alkalinity values determined by different titration methods. Excess alkalinity also invalidates the assumptions applied to marine CO₂ system calculations, and so would produce incorrect values of CO₂ system parameters calculated from certified total alkalinity and dissolved inorganic carbon values of CRMs. Finally, excess alkalinity analyses highlight the urgent need for the marine chemistry community to establish a universally agreed upon total boron to salinity ratio.

1. Introduction

The changes in ocean chemistry that have been induced by an influx of carbon dioxide (CO₂) to the ocean–atmosphere system from fossil fuel burning and land use change (Friedlingstein et al., 2019) have been well-documented (Caldeira and Wickett, 2003; Feely et al., 2004; Orr et al., 2005). The total amount of dissolved inorganic carbon in the ocean is increasing, causing an increase in hydrogen ion concentration (i.e., ocean acidification), a decrease in carbonate ion concentration, and myriad associated effects on marine organisms.

Chemical changes to the ocean are monitored in part by measuring parameters of the marine carbonate system. These parameters include total alkalinity (A_T), total dissolved inorganic carbon (C_T), the negative logarithm of the hydrogen ion concentration (pH), and the fugacity of CO₂ (f_{CO_2}). Standard operating procedures (SOPs) have been detailed for measurement of each of these parameters (Dickson et al., 2007).

Seawater A_T is defined as the total moles of hydrogen ions equal to the excess of proton acceptors over proton donors in one kilogram of

seawater (Dickson, 1981). Proton acceptors are defined as bases formed from weak acids with a pK^0 greater than 4.5, whereas proton donors are defined as weak acids with a pK^0 less than 4.5. Seawater A_T is typically described by the following equation (Dickson, 1981; Wolf-Gladrow et al., 2007):

$$A_T = [\text{HCO}_3^-] + 2[\text{CO}_3^{2-}] + [\text{B(OH)}_4^-] + [\text{OH}^-] + [\text{HPO}_4^{2-}] + 2[\text{PO}_4^{3-}] + [\text{SiO(OH)}_3^-] + [\text{HS}^-] + 2[\text{S}^{2-}] + [\text{NH}_3^+] + \dots - [\text{H}^+]_f - [\text{HSO}_4^-] - [\text{HF}^0] - [\text{H}_3\text{PO}_4^0] - \dots \quad (1)$$

where brackets represent total ion concentrations and subscript f denotes the free H⁺ concentration. The ellipses represent additional proton acceptors and donors that are not explicitly included in the equation.

Seawater C_T is simply the total moles of dissolved inorganic carbon in one kilogram of seawater, described by:

$$C_T = [\text{CO}_2^*] + [\text{HCO}_3^-] + [\text{CO}_3^{2-}] \quad (2)$$

* Corresponding author.

E-mail address: rbyrne@usf.edu (R.H. Byrne).

where brackets again represent total ion concentrations and $[CO_2^*]$ is equal to the sum of dissolved CO_2 and carbonic acid: $[CO_2^*] = [CO_2(aq)] + [H_2CO_3^0]$.

Those two parameters — A_T and C_T — are invariant with changes in temperature and pressure when defined in terms of moles per kilogram of seawater, and can be preserved in a sample for a long period of time if the sample is properly stored. Because of this behavior, certified reference materials (CRMs) with verified values of A_T and C_T have been produced for the last three decades (Dickson, 2010) at Scripps Institution of Oceanography (SIO).

CRMs are prepared from natural seawater collected off the coast of Southern California (Dickson, 2010). That seawater is filtered, sterilized with ultraviolet radiation, poisoned with a saturated solution of mercuric chloride ($HgCl_2$) to suppress biological activity, collected into clean borosilicate bottles, and certified for A_T and C_T . Each bottle is sealed with a glass stopper, Apiezon® L grease, and a tightly applied rubber band. Along with detailed SOPs, CRMs have been instrumental in improving consistency in A_T and C_T measurements over time and between different research groups (Bockmon and Dickson, 2015; Dickson, 2010; Olsen et al., 2019).

In an effort to characterize the ratio of total boron to salinity in seawater (r_B), we designed a novel acidimetric titration approach, taking advantage of the fact that a form of boron — borate ($[B(OH)_4^-]$) — contributes to A_T in seawater. This work was motivated by the fact that the two values of r_B most commonly used by the marine chemistry community (Uppström, 1974; Lee et al., 2010) — which were both determined using curcumin-based methods (Uppström, 1968; Liu and Lee, 2009) — differ by about 4%. Our goal was to obtain an independent measure of r_B using a method unrelated to the curcumin method.

For this purpose, seawater from the surface Gulf of Mexico (GoM) was collected and three different batches of CRM were acquired (batch 172, 176, and 183). Titrations were performed in near-absence of CO_2 using coulometrically standardized HCl (Dickson et al., 2003). Each titration was initiated from a pH as near as possible to the negative logarithm of the boric acid dissociation constant (pK_B) of the sample. At this condition, borate concentration ($[B(OH)_4^-]$) is equal to half the total boron concentration (B_T).

As a result of these titrations, however, a consistent r_B value was not obtained. Rather, most of our measurements indicated a prevalence of excess alkalinity. Moreover, a repeated difference between excess alkalinity in CRM batches and in open-ocean seawater from the Gulf of Mexico was noted. “Excess alkalinity” refers to an alkalinity contribution that is not attributable to inorganic bases included in the traditional definition of seawater total alkalinity (i.e., from Dickson, 1981). Excess alkalinity values were greater for the CRMs than for the GoM seawater, and appeared to differ between certain CRM batches.

We interpret excess alkalinity to be most probably associated with unidentified dissolved organic bases that bind protons during the course of a titration (e.g., Brewer et al., 1986; Bradshaw and Brewer, 1988; Cai et al., 1998; Hernández-Ayón et al., 1999, 2007; Kim and Lee, 2009; Yang et al., 2015), and that persist despite the ultraviolet irradiation step of CRM preparation. However, the analyses detailed here provide no definitive connection between excess alkalinity values and any dissolved organic bases, so we maintain the “excess alkalinity” terminology throughout this note rather than using “organic alkalinity.”

Excess alkalinity (A_X) invalidates typically assumed relationships between A_T and other carbonate system parameters, potentially contributing to thermodynamic inconsistency in marine carbonate system datasets (e.g., Fong and Dickson, 2019). The prevalence of A_X in CRMs has been suspected (Andrew Dickson, personal communication), but not robustly demonstrated until now. A_X in CRMs has the potential to cause errors in both CRM-based quality control of A_T measurements and CRM-based derivations of CO_2 system parameters (e.g., pH, f_{CO_2} , etc.).

2. Methods

2.1. Pre-treatment of samples

Seawater from the surface GoM was collected from a towed surface flow-through system into a large polyethylene carboy on 4 February 2020, from the *R/V Weatherbird II* near 26° N, 84° W. No additional processing of the seawater was conducted on the ship. The seawater carboy was stored in a mostly dark laboratory for at least one month prior to measurements being made, allowing for any large particles to settle and possibly for heterotrophic remineralization to break down any organic material. Subsamples were siphoned from the center of this large carboy.

Seawater from an SIO CRM batch or the GoM carboy was collected into a 1 L bottle, then acidified with 1 M HCl to a pH between about 3.0 and 3.5. This acidified seawater was purged of CO_2 for ~ 1 h using a stream of ultra-high purity N_2 passed through a column of Ascarite II CO_2 absorbent (Thomas Scientific). Ancillary experimentation indicated that this process raises sample salinity by 0.039 ± 0.016 ($n = 9$). This salinity increase was accounted for in calculations and the standard deviation used to inform the uncertainty estimate for salinity (Section 2.6). After bubbling with N_2 , the bottle was sealed tightly using a cap with integrated valves for gas input and solution output.

Headspace pressure was applied with N_2 to force about 150 mL of seawater into an open-top glass cell that was placed in a cell holder thermostatted to 18° C and positioned within the light path of an Agilent 8453 UV-visible spectrophotometer. The temperature of 18° C was chosen as a practical compromise between stability of temperature control in a room-temperature laboratory and limitation of the uncertainty contribution from the dissociation constant of water (K_W), which is lower at lower temperatures. Submerged in the sample were a plastic stirrer, a temperature probe, and a glass ROSS™ combination pH electrode (model 8102BN, Orion™) connected to a pH meter (model 720A, Orion™). An atmosphere of high-purity N_2 was maintained over the cell; the atmosphere was confirmed to be CO_2 -free using a LI-7000 CO_2/H_2O Analyzer (LI-COR Biosciences).

The method then proceeded in two steps, which were repeated a number of times for each seawater sample. Fig. 1 provides an overview of the measurement procedure, which is described in detail in the following paragraphs.

2.2. Identification of R_{pKB}

The first step of the experimental procedure involved identifying the absorbance ratio of a pH indicator dye that corresponded to the apparent dissociation constant of boric acid (pK_B) for each sample at 18° C (Fig. 1). We used thymol blue (TB; Zhang and Byrne, 1996) due to its optimal indicating range of approximately $7.5 < pH_T < 8.9$. Absorbance ratios (R) for TB are determined by:

$$R = (A_{596} - A_{750}) / (A_{435} - A_{750}) \quad (3)$$

where A_n is absorbance measured at wavelength n . pH_T is calculated via an equation of the form:

$$pH_T = -\log\{K_2e_2\} + \log\{(R - e_1) / (1 - R \cdot e_3/e_2)\} \quad (4)$$

where K_2 is the dissociation constant of the H_2I^- form of the indicator dye and e_x terms are molar absorption ratios defined as follows (Zhang and Byrne, 1996):

$$e_1 = \frac{596\epsilon_{HI}}{435\epsilon_{HI}} \quad (5a)$$

$$e_2 = \frac{596\epsilon_I}{435\epsilon_{HI}} \quad (5b)$$

$$e_3 = \frac{435\epsilon_I}{435\epsilon_{HI}} \quad (5c)$$

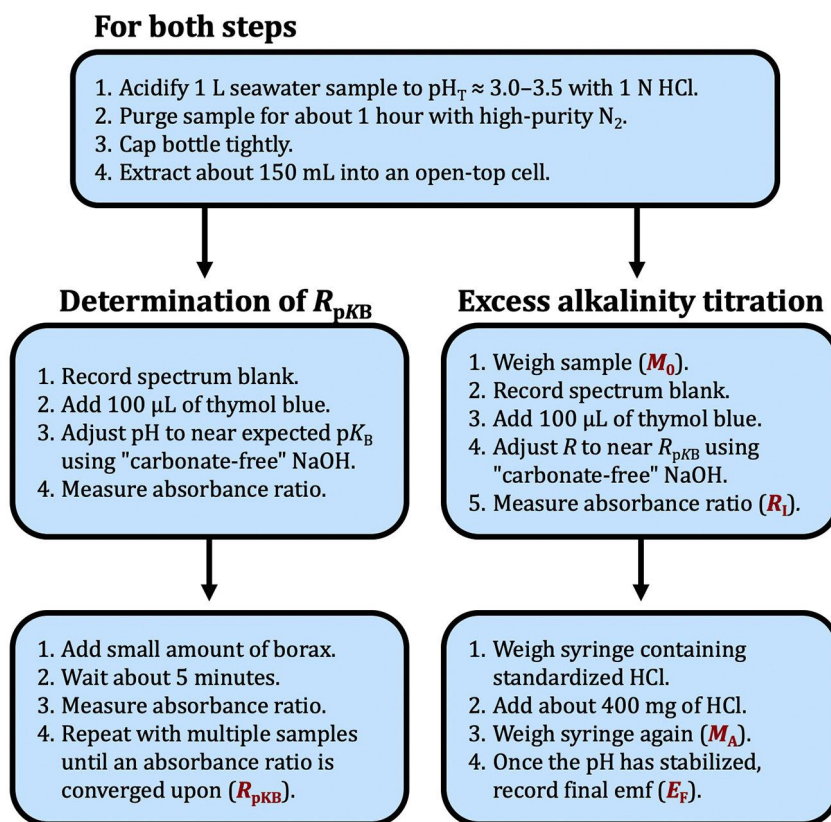


Fig. 1. The two steps of the experimental procedure are detailed here. Important measured quantities are bold and red in color. (For interpretation of the references to color in this figure legend, the reader is referred to the web version of this article.)

where $\lambda\epsilon_k$ is the molar absorbance coefficient of species k at wavelength λ .

Though a purification process for TB has been developed (Hudson-Heck and Byrne, 2019), we used unpurified dye for this work. The congruence between pK_2 values of TB determined using purified versus unpurified TB (Hudson-Heck and Byrne, 2019) and determined by different investigators using unpurified TB obtained from different vendors (Mosley et al., 2004) indicates that the effect of impurities on pH_T measured with TB is small. Further, our uncertainty analysis suggests that quantitative inaccuracy in measurements of initial pH_T is not a significant uncertainty contributor to our results (see Section 3).

A spectrophotometer blank was taken before adding 100 μ L of 10 mM TB to the seawater. Then, “carbonate-free” NaOH (1 M) was added to adjust the seawater pH to near the pK_B value. “Carbonate-free” NaOH was prepared by treating NaOH with $\text{CaO}_{(s)}$ in a sealed bottle to precipitate calcium carbonate (Sipos et al., 2000), then allowing particles to settle for 48–72 h. Using a 50 μ L gastight syringe (Hamilton Company), NaOH was extracted from the center of the bottle to avoid contamination from particles.

Finally, sodium borate decahydrate ($\text{Na}_2\text{B}_4\text{O}_7 \cdot 10\text{H}_2\text{O}$; borax) was added to the seawater, forming boric acid ($\text{B}(\text{OH})_3$) and borate ($\text{B}(\text{OH})_4^-$), thus causing the pH of the seawater to trend toward the pK_B .

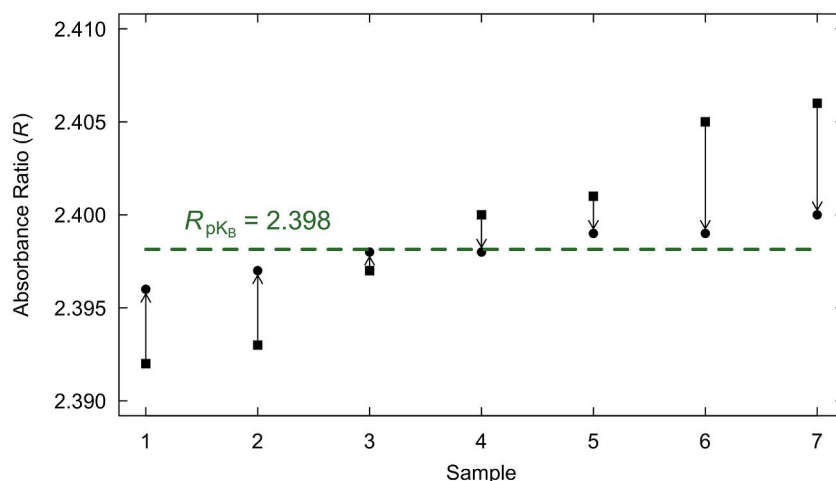


Fig. 2. Identification of a sample's absorbance ratio corresponding to its pK_B value (R_{pKB}). The squares represent R after an initial pH adjustment with “carbonate-free” NaOH, the arrows ending at the circles represent the changes in R upon addition of borax, and the dotted line represents the R_{pKB} .

Five absorbance spectra were taken before and after addition of borax for calculation of R (Eq. (3)). This process was repeated with several subsamples from the 1 L bottle to achieve convergence toward the absorbance ratio at which the pH of the sample was equal to its pK_B (i.e., R_{pK_B}). Fig. 2 demonstrates the logic behind this first step.

2.3. Excess alkalinity titration

The second step of the experimental procedure involved acidimetric titration starting from $pH = pK_B$ (Fig. 1). This step was designed to measure borate alkalinity for easy calculation of B_T (for direct determination of r_B). However, early results indicated persistent excess alkalinity, suggesting that isolation of borate alkalinity alone would be impossible. So, the titration starting point (i.e., $pH = pK_B$) instead allowed for measurement of the magnitude of borate alkalinity plus any other excess alkalinity source.

Seawater was weighed upon addition to the open-top cell. Again, a spectrophotometer blank was taken before adding 100 or 150 μ L of 10 mM TB to the seawater. The dilution effect by the indicator dye solution on total constituent concentrations and the indicator alkalinity effect (Li et al., 2020) were both accounted for. However, the perturbation from initial sample pH was not corrected for, because calculations relevant to the excess alkalinity titration require knowledge of the solution pH at each step, not the pH of the unadjusted sample.

Next, “carbonate-free” NaOH (1 M) was added to adjust the seawater absorbance ratio as near as possible to R_{pK_B} . An initial absorbance ratio (R_I) was measured, along with the electromotive force (emf) at initial conditions (E_I), both for calculation of initial pH_T (pH_I) in the adjusted sample with dye solution added. Finally, certified HCl titrant (Dickson et al., 2003) with a concentration of 0.100362 mol kg^{-1} (± 0.000009 mol kg^{-1} ; Batch A17) was used to titrate the seawater to a pH between about 4.4 and 5.0. The emf measured via glass pH electrode after the titration was recorded (E_F) for calculation of final pH_T (pH_F). This process was repeated with several subsamples from each 1 L bottle.

2.4. Calculations of borate alkalinity and excess alkalinity

Borate alkalinity (A_B) and excess alkalinity (A_X) were calculated by:

$$A_{B+X} = A_B + A_X = A_T - A_C - A_m \quad (6)$$

where A_{B+X} is the combination of equilibrium borate alkalinity and excess alkalinity, A_T is the total alkalinity determined from each titration, A_C is the carbonate alkalinity, and A_m is the alkalinity contributed by “minor components” such as nutrients, hydroxide ions, and the thymol blue indicator. The distinction of A_B as “equilibrium” borate alkalinity means A_B is equal to $[B(OH)_4^-]$ at $pH = pK_B$. This treatment allows for direct comparison of salinity-normalized A_{B+X} values between different samples, the advantages of which are discussed later. Carbonate alkalinity (A_C) was minimized by purging CO_2 from acidified samples using high-purity N_2 (Section 2.1).

The full derivation of Eq. (6) is given in Appendix A; the A_T , A_C , and A_m terms are summarized below. In each of the following equations, total solute concentrations for calculations of individual species were either estimated from salinity (F_T , B_T) or from direct measurements (P_T , S_T , C_T).

Total alkalinity, A_T , is determined by:

$$A_T = \frac{M_A C_A - M_T ([H^+]_F + [HF^0]_F - [HCO_3^-]_F - [HPO_4^{2-}]_F - [B(OH)_4^-]_F - [OH^-]_F - [I^{2-}]_F + [H_3PO_4^0]_F)}{M_0} \quad (7)$$

where M_0 is the initial sample mass, M_A is the added acid mass, M_T is equal to M_0 plus M_A , C_A is the acid concentration, and $[x]_F$ represents the final concentration of species x at the titration endpoint. Species with concentrations less than 1 nmol kg^{-1} at the titration endpoint (e.g., $[CO_3^{2-}]$ and $[PO_4^{3-}]$) are treated as negligible.

I^{2-} is the deprotonated form of TB indicator dye, which contributes positively to A_T (Li et al., 2020). The concentration of I^{2-} is calculated by treating HI^- as a monoprotic weak acid: $[I^{2-}] = I_T / (1 + [H^+] / K_{12})$, where I_T is the total TB concentration and K_{12} is calculated using the equation of Zhang and Byrne (1996). HI^- can be reasonably treated as a monoprotic acid because the first dissociation constant of TB (pK_1) is a few orders of magnitude lower than the final pH of our excess alkalinity titrations ($pK_1 \approx 1.5$; King and Kester, 1989).

All values of $[x]_F$ were calculated from pH_F , which was determined using E_F and the equation:

$$pH_T = (E - E_0) / (RT \cdot \ln(10) / F) \quad (8)$$

where E is the measured emf, E_0 is the electrode intercept potential, R is the ideal gas constant, T is temperature in Kelvin, and F is the Faraday constant.

Glass electrodes used to measure emf were periodically confirmed to give a Nernstian response by titration of 0.7 M NaCl with HCl. Once the expected response was confirmed, the ideal Nernstian slope ($RT \cdot \ln(10) / F$) was used. One-point calibrations were performed prior to each seawater titration using the pH_T measurement provided by thymol blue, similar to the one-point mCP calibrations discussed by Easley and Byrne (2012). The electrode intercept potential (E_0) was adjusted slightly so that pH_I measured using Eq. (4) with R_I matched pH_I measured using Eq. (8) with E_I .

Alkalinity contributed by bicarbonate and carbonate, A_C , is determined by:

$$A_C = [HCO_3^-]_I + 2[CO_3^{2-}]_I = \frac{C_T K_1 ([H^+]_I + 2K_2)}{[H^+]_I^2 + K_1 [H^+]_I + K_1 K_2} \quad (9)$$

where C_T is experimentally estimated (see Section 2.5). Alkalinity contributed by minor components, A_m , is determined by:

$$A_m = [OH^-]_I + [I^{2-}]_I + 2[PO_4^{3-}]_I + [HPO_4^{2-}]_I + [SiO(OH)_3^-]_I - [H^+]_I + [B(OH)_4^-]_{ex} \quad (10)$$

In Eqs. (9) and (10), $[x]_I$ represents the initial concentration of species x at the start of the titration. Species with concentrations less than 1 nmol kg^{-1} at the initial pH (e.g., $[HF^0]$ and $[H_3PO_4^0]$) are treated as negligible. Values of $[x]_I$ were calculated from pH_I , determined via thymol blue absorbance ratios (Eqs. (3)–(5)).

Phosphate and silicate species were determined using total phosphate (P_T) and silicate (S_T) concentrations, which were reported in the documentation for CRMs or measured spectrophotometrically using a flow injection analysis system (Parsons, 1984) for GoM seawater. Standard deviations between nutrient measurements performed on subsamples collected at different times from the GoM seawater carboy were used to inform uncertainty estimates for nutrient concentrations.

$[B(OH)_4^-]_{ex}$ is a measure of the degree to which the initial borate concentration ($[B(OH)_4^-]_I$) was greater than (+) or less than (–) the borate equilibrium value ($[B(OH)_4^-]_{eq}$) at the start of the titration:

$$[\text{B(OH)}_4^-]_{\text{ex}} = [\text{B(OH)}_4^-]_1 - [\text{B(OH)}_4^-]_{\text{eq}} = B_T \left/ \left(1 + \frac{[\text{H}^+]_1}{K_B} \right) \right. - B_T \left/ \right. 2 \quad (11)$$

$[\text{B(OH)}_4^-]_{\text{ex}}$ was calculated using an average of B_T estimated from Uppström (1974) and from Lee et al. (2010) and was generally between -2.0 and $+2.0 \mu\text{mol kg}^{-1}$. Including $[\text{B(OH)}_4^-]_{\text{ex}}$ in the A_m term allows for $A_{\text{B}+X}$ values to be directly compared between samples with identical salinity, and for salinity-normalized $A_{\text{B}+X}$ values to be directly compared between any two samples.

Because $\text{pH} = \text{p}K_B$ was independently determined, uncertainty in the salinity- and temperature-dependent characterization of $\text{p}K_B$ (Dickson, 1990) was circumvented. Further, any minor changes to $\text{p}K_B$ induced by interactions between boric acid and bicarbonate (McElligott and Byrne, 1998; Mojica Prieto and Millero, 2002) or boric acid and dissolved organics (Mackin, 1986) would be accounted for by this method.

To obtain excess alkalinity (A_X), the A_B component had to be subtracted from $A_{\text{B}+X}$ (Eq. (6)). The A_B component was determined using both the r_B ratio of Uppström (1974) and of Lee et al. (2010), each of which provide a different value of A_X .

2.5. C_T measurements

To account for residual dissolved CO_2 , a custom-built gas extraction system coupled to a Picarro G5131-i cavity ringdown spectrometer for CO_2 quantification was used to measure the C_T of the N_2 -purged seawater samples ($C_{T(\text{samp.})}$) and the NaOH titrant solution ($C_{T(\text{NaOH})}$). The system has demonstrated good precision for seawater C_T measurements made in our laboratory, comparable to that of a coulometer ($\pm 0.1\%$; X. Liu, unpublished data). For the purposes of this study (i.e., C_T measurements of nearly CO_2 -free samples), the standard deviations between duplicate samples given in Table B3 can provide some idea of the system's precision ($\pm 0.15 \mu\text{mol kg}^{-1}$).

For C_T measurements of the seawater samples, N_2 headspace pressure was applied after purging to force $\sim 230 \text{ mL}$ of solution into a glass BOD bottle under an N_2 atmosphere. For C_T measurements of the NaOH solution, Milli-Q water was heated and bubbled with high-purity N_2 as it cooled to remove dissolved CO_2 . Then, N_2 headspace pressure was applied to force $\sim 230 \text{ mL}$ of Milli-Q water into a glass BOD bottle under an N_2 atmosphere. To half of the Milli-Q-filled flasks, $150 \mu\text{L}$ of "carbonate-free" NaOH was added, whereas half consisted of CO_2 -purged Milli-Q water only. All these bottles were rapidly sealed with greased glass stoppers.

Each sample was acidified and the evolved CO_2 run through a Picarro G5131-i cavity ringdown spectrometer to measure C_T . For each sample run, an acid blank was measured to serve as a zero C_T "standard" and an unmanipulated CRM was measured to establish a linear relationship between system "counts" and C_T . The average $C_{T(\text{samp.})}$ was used as an estimate for residual C_T in each sample after purging. The difference between the C_T of NaOH -spiked Milli-Q and pure Milli-Q was used to determine the added $C_{T(\text{NaOH})}$ per μL of "carbonate-free" NaOH . The accuracy of these C_T measurements, estimated by repeated measurements across different samples collected at different times, was accounted for in the uncertainty analysis detailed in the following section.

2.6. Uncertainty analysis

A comprehensive uncertainty analysis was performed to assign a standard uncertainty to the A_X results. This was done by propagating standard uncertainties in measured values using a Gaussian approach (Ellison and Williams, 2012):

$$u_c^2(A_X) = \left(\frac{\delta(A_X)}{\delta x_1} \right)^2 u^2(x_1) + \dots + \left(\frac{\delta(A_X)}{\delta x_n} \right)^2 u^2(x_n) \quad (12)$$

where $\frac{\delta(A_X)}{\delta x_n}$ is the change in A_X for a given change in input variable x_n , $u(x_n)$ is the standard uncertainty in input variable x_n , and $u_c(A_X)$ is the combined standard uncertainty in A_X . Uncertainty in r_B was not included in this analysis, and is instead addressed by directly comparing A_X values determined via the Uppström (1974) r_B versus the Lee et al. (2010) r_B .

Non-parametric pairwise analysis of variance (ANOVA) was used to assess differences between the mean A_X values of different sample types. The FATHOM toolbox for MATLAB® was used for this analysis (Jones, 2017). To test significance, p values were determined by a permutation test ($n = 10,000$) and corrected for multiple comparisons using Holm's correction (Holm, 1979).

The statistical test was first run directly on measured A_X values. Then, in a Monte Carlo error analysis, simulated uncertainty was added to each measurement of A_X using a normal distribution centered around zero with a standard deviation equal to $u_c(A_X)$. The non-parametric pairwise ANOVA was run 10,000 times with this added uncertainty, and resulting p values were interpreted.

3. Results

Table 1 shows the properties of each measured sample, including the $R_{\text{p}K_B}$ values determined by the methodological step described in Section 2.2. Full titration data are given in Table B1 of Appendix B, and a summary of results is given in Table B2.

Fig. 3. shows $C_{T(\text{samp.})}$ measurements that were made on purged seawater samples (Table B3), most of which were below $4.0 \mu\text{mol kg}^{-1}$ ($1.7 \pm 1.9 \mu\text{mol kg}^{-1}$, $n = 12$). For the NaOH titrant, pairs of NaOH -spiked Milli-Q water and pure Milli-Q water gave a carbonate content of 5.7 ± 1.7 nanomoles C_T per μL titrant ($n = 6$, Table B4). This value was used with the amount of NaOH added to each sample in μL to estimate the added $C_{T(\text{NaOH})}$ in $\mu\text{mol kg}^{-1}$ (e.g., $100 \mu\text{L}$ NaOH added to 150 g of seawater increases C_T by $3.8 \pm 1.3 \mu\text{mol kg}^{-1}$).

Added $C_{T(\text{NaOH})}$ was used with the average $C_{T(\text{samp.})}$ to represent the total C_T present in titrated samples during calculations of A_X . This resulted in about $5.0\text{--}7.0 \mu\text{mol kg}^{-1}$ C_T per sample. The standard deviations across all $C_{T(\text{samp.})}$ and $C_{T(\text{NaOH})}$ measurements were used to represent standard input uncertainties for the uncertainty analysis.

Salinity-normalized values of $A_{\text{B}+X}$ ($nA_{\text{B}+X}$) are shown in **Fig. 4**. These were determined according to Eq. (6), and normalized to $S = 35$ to account for salinity-dependent differences in total boron concentrations between the samples. This normalization allows $nA_{\text{B}+X}$ to be directly compared between samples. However, normalizing the entire $A_{\text{B}+X}$ quantity does misleadingly imply that A_X , like A_B , is proportional to salinity. Also, because $nA_{\text{B}+X}$ values are representative of $\text{pH} = \text{p}K_B$, the A_B component is much larger than it would be for a sample at its natural pH.

To isolate A_X , two different total boron to salinity ratios were applied to account for A_B . **Fig. 5a** shows A_X determined using the r_B of Uppström (1974) and **Fig. 5b** shows A_X determined using the r_B of Lee et al. (2010). Because the Lee et al. ratio ($0.1336 \text{ mg kg}^{-1\% \text{oo}^{-1}}$, $B_T = 432.6 \mu\text{mol kg}^{-1}$ at $S = 35$) is larger than the Uppström ratio ($0.1284 \text{ mg kg}^{-1\% \text{oo}^{-1}}$, $B_T = 415.8 \mu\text{mol kg}^{-1}$ at $S = 35$), A_B makes up a greater proportion of $A_{\text{B}+X}$ when calculated using the Lee et al. ratio. For this reason, A_X values calculated using Lee et al. ratio are smaller than those calculated using the Uppström ratio.

Table 1

Properties of different measured seawater samples. Salinity before purging with N_2 (S), total phosphate concentration (P_T), total silicate concentration (Si_T), and absorbance ratio at $\text{pH} = \text{p}K_B$ ($R_{\text{p}K_B}$) are provided for each.

Sample type	S	P_T	Si_T	$R_{\text{p}K_B}$
Surface GoM	36.286	0.21	1.7	2.311
CRM 172	33.450	0.42	2.8	2.386
CRM 176	33.532	0.29	1.7	2.365
CRM 183	33.420	0.35	2.1	2.372

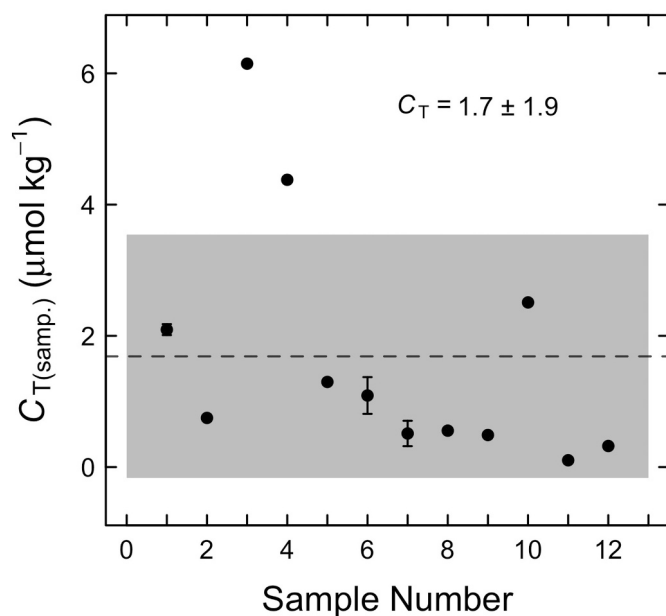


Fig. 3. Dissolved inorganic carbon ($C_{T(samp)}$) in acidified seawater samples that had been purged for ~ 1 h with high-purity N_2 gas. Measurements are displayed in the order of analysis. The dashed line and grey rectangle represent the mean and standard deviation of the measurements, respectively. Data points that are averages of duplicate measurements include errors bars representing the standard deviation between the two measurements.

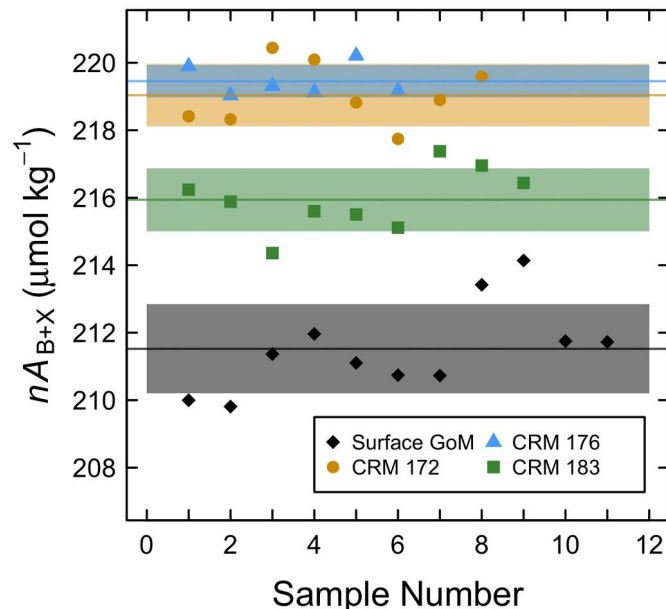


Fig. 4. Salinity-normalized values of A_{B+X} (nA_{B+X}) for surface GoM seawater, CRM 172, CRM 176, and CRM 183. The colored lines and shaded rectangles represent the means and standard deviations for each sample type. Sample number represents the order in which samples of each given type were measured.

Combined standard uncertainty in A_X ($u_c(A_X)$) was estimated by propagating input uncertainties for a model sample titration. Table 2 shows the main input parameters that contribute to A_X uncertainty. Uncertainty in r_B was not considered because we explicitly discuss differences caused by using either the Uppström (1974) or Lee et al. (2010) ratio.

The most important input uncertainties are associated with residual

C_T after purging ($C_{T(samp)}$) and added with the NaOH titrant ($C_{T(\text{NaOH})}$). These uncertainties were estimated as the standard deviations of repeated C_T measurements (Tables B3 and B4).

Uncertainty in final pH_T was estimated at 0.01 based on the rather conservative estimate of “total uncertainty” in pH given by Orr et al. (2018). The final pH_T uncertainty is a somewhat important contributor; however, its influence is lessened by the high pH at which the titration is terminated. The relatively high pH ($\text{pH}_T \approx 4.4\text{--}5.0$) limits the $[\text{H}^+]_F$ term in Eq. (7) to about 10–40 $\mu\text{mol kg}^{-1}$.

Uncertainty in R_{pKB} was estimated from repetitions of the process for identifying R_{pKB} , which is detailed in Section 2.2. Uncertainty in R_{pKB} influences estimates of excess borate ($[\text{B(OH)}_4^-]_{\text{ex}}$) at the titration starting point.

Uncertainty in pK_W (0.01) was taken from the estimate of Orr et al. (2018). The A_X uncertainty that is attributable to pK_W uncertainty is influenced by the temperature at which the titration is carried out. For example, $(\delta(A_X)/\delta\text{pK}_W)^2 \cdot u^2(\text{pK}_W)$ changes from $0.12 \mu\text{mol}^2 \text{kg}^{-2}$ at 18°C to $0.30 \mu\text{mol}^2 \text{kg}^{-2}$ at 25°C .

Uncertainty in M_A was estimated as 5 times the resolution of the balance used for M_A measurements. Uncertainty in M_A is the smallest contributor listed here, partly due to the relative precision with which M_A can be measured.

Pairwise ANOVA tests conducted on directly measured A_X values for each sample type indicated a significant difference between each group ($p = .001$), except for CRM 172 versus CRM 176 (Table 3). (To account for multiple comparisons, p values were corrected using Holm's correction (Holm, 1979).)

When simulated uncertainty based on the $u_c(A_X)$ estimate ($2.8 \mu\text{mol kg}^{-1}$; Table 2) was added to measured A_X values for the Monte Carlo error analysis, pairwise ANOVA tests indicated significant p values (i.e., $p < .05$) for more than 55% of simulations for all comparisons of CRMs to GoM seawater, and for more than 95% of simulations for comparisons of CRM 172 and CRM 176 to GoM seawater (Table 3). However, comparisons among CRM groups were not consistently significant at a level of $\alpha = 0.05$ when simulated uncertainty was considered.

4. Discussion

4.1. Excess alkalinity in CRMs

Fig. 5 indicates an alkalinity excess in CRMs that is greater than the alkalinity excess found in GoM seawater ($p = .001$) by between 3.9 and $7.4 \mu\text{mol kg}^{-1}$ (Table B2). This alkalinity excess may vary to a small degree between CRM batches, despite the fact that the p values are not consistently significant (at a level of $\alpha = 0.05$) when uncertainty is simulated (Table 3). The absolute value of A_X in each sample type is somewhat uncertain due to experimental uncertainties, primarily those associated with the residual C_T estimates and the value of r_B . The negative A_X values that result in certain cases when the Lee et al. (2010) r_B is used to account for borate alkalinity (Fig. 5b) suggest that the Lee et al. (2010) estimate of r_B in seawater may be too high. Alternatively, experimental uncertainties may have combined to produce A_{B+X} values (Fig. 4) that were anomalously low. Despite uncertainty in the absolute values of A_X , the difference between A_X in the CRMs versus the GoM seawater is repeatable and robust. The most plausible explanation for this repeatable difference, in our estimation, is a small amount of excess alkalinity in the CRM batches we analyzed.

There are a few possible explanations for excess alkalinity being present at higher levels in CRMs than in the GoM seawater we collected. First, the nature of the marine environment off the coast of California (where seawater for CRM preparation is collected) promotes high biological productivity and therefore high concentrations of dissolved organic material, which can accept protons during titration (Cai et al., 1998; Hernández-Ayón et al., 2007; Kim and Lee, 2009; Muller and Bleie, 2008). This organic material should be partially broken down by

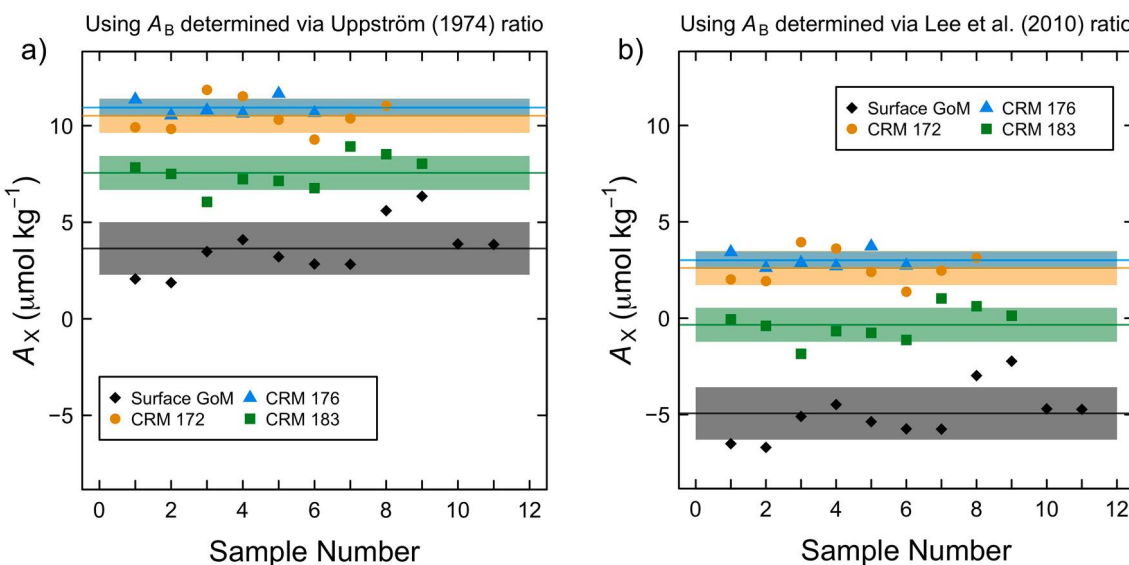


Fig. 5. Values of A_X determined by applying the total boron to salinity ratio of (a) Uppström (1974) and (b) Lee et al. (2010) to calculate A_B to subtract from A_{B+X} . The colored lines and shaded rectangles represent the means and standard deviations for each sample type. Sample number represents the order in which samples of each given type were measured.

Table 2

Uncertainties in input parameters for the calculation of A_X and their propagation to combined standard uncertainty in A_X in $\mu\text{mol kg}^{-1}$; calculated using Eq. (12). These were determined using a model titration of seawater with $S = 35$, $t = 18^\circ\text{C}$, $M_0 = 150$ g, and $M_A = 400$ mg.

Parameter (x)	x (approx.)	$u(x)$	$\delta(A_X)/\delta x$	$(\delta(A_X)/\delta x)^2 \cdot u^2(x)$	$u(A_X)$ ($\mu\text{mol kg}^{-1}$)
$C_{T(\text{samp.})}$ ($\mu\text{mol kg}^{-1}$)	1.7	1.9	1.2	5.2	1.8
$C_{T(\text{NaOH})}$ ($\text{nmol } \mu\text{L}^{-1}$)	5.7	1.7	0.8	1.9	0.7
pH_F	4.622	0.010	-56.8	0.3	0.1
R_{pKB}	2.410	0.010	-51.7	0.3	0.1
$pK_W(18^\circ\text{C})$	13.50	0.01	-34.4	0.1	0.0
M_A (g)	0.4000	0.0005	-668.0	0.1	0.0
			$u_c(A_X)$ ($\mu\text{mol kg}^{-1}$)		2.8

Uncertainties in other input parameters were considered and used in the calculation of $u_c(A_X)$, but are not listed here as their contributions were quite small. A comprehensive accounting of uncertainties as well as rationale for each input uncertainty estimate is given in Table B5.

the UV irradiance step of CRM preparation. However, the level of UV light applied during this step may be sufficient only to suppress active biological processes and not to completely destroy all organic material (Andrew Dickson, personal communication). Second, though the GoM seawater was not explicitly irradiated like CRM batches, it was collected from very near the surface. So, UV irradiation from the natural environment could have played a role in breaking down organic matter before collection of the sample. Further, the storage of the sample in a mostly dark laboratory may have allowed for additional heterotrophic breakdown of any organic material that was present, leading to a decrease in excess alkalinity.

The excess alkalinity values presented here are not exactly equivalent to those that would appear in standard alkalinity titrations, though they are likely very similar. That is because our titrations were initiated from $\text{pH} = pK_B$ ($\text{pH}_T \approx 8.6\text{--}8.7$) and terminated at $\text{pH}_T \approx 4.4\text{--}5.0$; typical alkalinity titrations are initiated from natural seawater pH ($\text{pH}_T \approx 7.2\text{--}8.2$) and terminated at $\text{pH}_T \approx 3.0\text{--}4.2$, depending on the method of titration. In theory, knowledge of the dissociation behavior of any organic acids contributing to excess alkalinity would be necessary to translate A_X values obtained using the method detailed here to those that

Table 3

Results of non-parametric pairwise ANOVA tests. Tests were performed on A_X values calculated using both the Uppström (1974) and Lee et al. (2010) r_B . p values are shown for comparisons with no simulated uncertainty ('no uncert.'), and percentages of p values that were less than .05 are shown for comparisons that included simulated uncertainty ('with uncert.'). All comparisons besides CRM 172 versus CRM 176 showed significant differences ($p = .001$) in measured A_X . With 10,000 simulations of uncertainty on A_X measurements, only comparisons of GoM versus CRM samples showed significant differences ($p < .05$) in more than 55% of simulations.

Comparison	A_X using Uppström (1974) r_B		A_X using Lee et al. (2010) r_B	
	p value (no uncert.)	Percent $p < .05$ (with uncert.)	p value (no uncert.)	Percent $p < .05$ (with uncert.)
GoM vs. CRM 172	.001	96.8%	.001	98.9%
GoM vs. CRM 176	.001	95.6%	.001	98.3%
GoM vs. CRM 183	.001	56.0%	.001	73.7%
CRM 172 vs. CRM 176	.311	2.3%	.336	2.3%
CRM 172 vs. CRM 183	.001	28.3%	.001	29.1%
CRM 176 vs. CRM 183	.001	32.0%	.001	31.7%

would be detected in a standard alkalinity titration.

4.2. Effect of A_X on CRM-based quality control of TA

The primary purpose of CRMs is to ensure historical and inter-laboratory consistency in A_T measurements. To achieve this goal, an A_T value that matches the certified value must be attainable for repeat measurements of a given CRM batch within an acceptable uncertainty range (e.g., $\pm 2 \mu\text{mol kg}^{-1}$). As long as any A_X component remains fairly constant over time (as it should in HgCl_2 -poisoned CRMs) there should be little to no differences between A_T values obtained during the CRM certification process and A_T values obtained during a given laboratory's quality control measures.

However, an assumption of the previous paragraph is that A_T must be determined exactly according to (or very similarly to) the titration protocol employed during the certification of A_T . This procedural

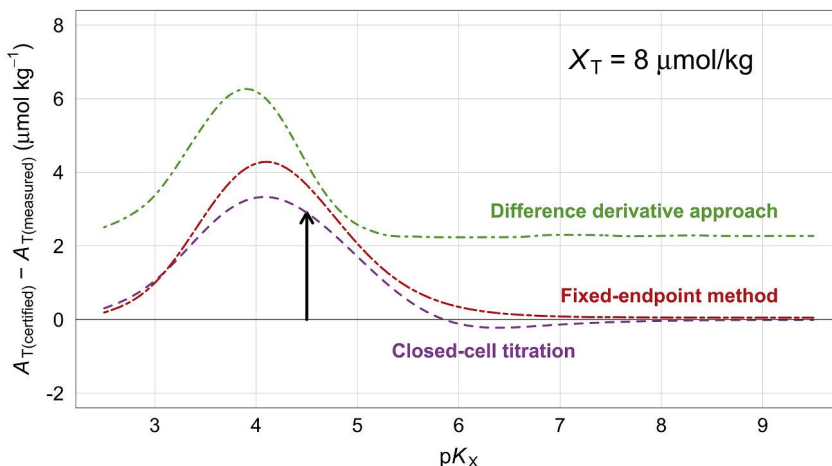


Fig. 6. Hypothetical differences between certified A_T values (Dickson et al., 2003) versus A_T values measured by closed-cell titrations (e.g., Millero et al., 1993), a fixed-endpoint method (e.g., Yao and Byrne, 1998), and a difference derivative approach (e.g., Hernández-Ayón et al., 1999) across a range of dissociation constants (pK_X) of a hypothetical excess alkalinity contributor (X_T). Values are determined using the model of Sharp and Byrne (2020), and solution characteristics are as follows: $S = 33.5$, $C_T = 2050.0$, $pH_T = 7.82$, $t = 20.0^\circ\text{C}$, $P_T = 0.5$, $Si_T = 2.0$.

similarity will ensure that the same amount of any excess proton acceptor is titrated during both A_T determinations. Potential differences in A_T values obtained via different titration methods in the presence of excess proton acceptors are explored by Sharp and Byrne (2020). Fig. 6 shows an example of how those methodology-based differences might manifest for A_T measurements of a CRM with an excess alkalinity contributor ($X_T = 8 \mu\text{mol kg}^{-1}$) across a range of dissociation constant values (pK_X).

As an example, consider a CRM with a certified A_T of $2199.0 \mu\text{mol kg}^{-1}$ ($S = 33.5$, $C_T = 2050.0$, $pH_T = 7.82$, $t = 20.0^\circ\text{C}$, $P_T = 0.5$, $Si_T = 2.0$), and imagine that CRM contains a dissolved organic acid with a total concentration of $8 \mu\text{mol kg}^{-1}$ and a $pK = 4.5$. Because CRMs are certified using an open-cell titration with data analysis performed via nonlinear fit (Dickson et al., 2003), the organic acid contributes $7.2 \mu\text{mol kg}^{-1}$ to the measured $2199.0 \mu\text{mol kg}^{-1}$ (determined via the 'TITRATE.m' model from Sharp and Byrne, 2020). If a laboratory used this CRM to verify its own closed-cell nonlinear fit procedure (e.g., Millero et al., 1993), they would obtain an A_T equal to $2196.1 \mu\text{mol kg}^{-1}$, assuming both titrations were performed perfectly. This may cause that laboratory to presume they have a systematic bias of $-2.9 \mu\text{mol kg}^{-1}$ in their A_T determinations (represented by the arrow in Fig. 6) when, in fact, the discrepancy was caused only by a difference in titration procedure.

Importantly, even if that $-2.9 \mu\text{mol kg}^{-1}$ bias were corrected for using the certified A_T value from the CRM — a practice that is common but not necessarily recommended (see Bockmon and Dickson, 2015) — seawater samples from the marine environment are not expected to contain the same amount of organic proton acceptors with the same characteristics as a given CRM. So, unexpected differences in measured A_T from that which would be obtained by the open-cell titration method used for certification of a CRM can still occur.

Table 4

Hypothetical differences (ΔpH_T) between calculated pH values ($pH_{\text{calc.}}$) and actual pH values (pH_{true}) of a CRM with a certified alkalinity of $2227.7 \mu\text{mol kg}^{-1}$ and a certified total dissolved inorganic carbon of $2040.0 \mu\text{mol kg}^{-1}$. The CRM includes a generic excess alkalinity contributor (X_T) with a given dissociation constant (pK_X), which produces a measured excess alkalinity (A_X) determined using the 'TITRATE.m' model (Sharp and Byrne, 2020). Calculations of $pH_{\text{calc.}}$ are made using CO2SYSv3.1 for MATLAB (Sharp et al., 2020), and calculations of pH_{true} are made using a modified version of CO2SYS v3.1 that allows for input of an additional protolyte (i.e., excess alkalinity contributor). Ancillary solution conditions are: $S = 33.5$, $t = 20^\circ\text{C}$, $P_T = 0.5 \mu\text{mol kg}^{-1}$, and $Si_T = 2.0 \mu\text{mol kg}^{-1}$.

A_T ($\mu\text{mol kg}^{-1}$)	C_T ($\mu\text{mol kg}^{-1}$)	X_T ($\mu\text{mol kg}^{-1}$)	pK_X	A_X ($\mu\text{mol kg}^{-1}$)	$pH_{\text{calc.}}$	pH_{true}	ΔpH_T
2227.7	2040.0	10.0	4.0	7.3	7.926	7.910	0.016
			5.0	9.6	7.926	7.905	0.021
			6.0	9.8	7.926	7.904	0.021
			7.0	8.9	7.926	7.907	0.019
			8.0	4.5	7.926	7.916	0.010
			9.0	0.8	7.926	7.924	0.002

Álvarez et al., 2020).

The presence of excess alkalinity in ocean waters is supported by thermodynamic consistency analyses of over-determined carbonate system datasets. Incongruence between calculated and measured carbonate system parameters is a recurring issue, as has been pointed out, for example, with regard to calculated versus measured pH (e.g., McElligott et al., 1998; Carter et al., 2013, 2018; Williams et al., 2017) and calculated versus measured f_{CO_2} at high f_{CO_2} (e.g., Lee et al., 2000; Lueker et al., 2000; Millero et al., 2002). Certain investigators have successfully remedied thermodynamic consistency issues by applying excess alkalinity corrections to measured alkalinity values (Millero et al., 2002; Patsavas et al., 2015; Fong and Dickson, 2019).

This notion that A_X values are non-negligible in seawater and vary spatially and temporally supports the application of measurement techniques like the titration procedure described here to full ocean profiles in order to account for and interpret A_X . Even more beneficial than the procedure described here may be some form of multi-step titration that not only measures A_X but provides an estimate of the charge groups that accept protons within a given pH range (e.g., Muller and Bleie, 2008; Yang et al., 2015; Ko et al., 2016). The reliability of excess alkalinity titrations may be improved by measurement of large-volume samples to reduce uncertainties associated with the amount of added acid and instability in residual C_T .

Uncertainties related to the value of r_B and the amounts of $C_{T(\text{samp})}$ and $C_{T(\text{NaOH})}$ do limit quantitative interpretations of excess alkalinity titrations. Still, reasonable estimates of A_X can be obtained when complicating factors are properly accounted for and interpretations are appropriately caveated in the context of measurement uncertainties (as is done here). Further, with consistent measurement conditions, comparisons between A_X values within a given dataset should be quite valuable.

4.5. Implications for the total boron to salinity ratio (r_B)

Our results highlight the degree to which the choice of r_B influences interpretations of alkalinity titrations and calculations of carbonate system parameters (see also, Woosley, 2021). The discrepancy between two commonly-employed ratios is magnified in our A_X results ($8\text{--}9 \mu\text{mol kg}^{-1}$), because our titrations start from $\text{pH} = \text{p}K_B$ — where A_B is 50% of B_T — rather than natural seawater pH_T — where A_B is about 10–25% of B_T . However, using one ratio over the other still produces significant differences in interpretations of A_T titrations and in calculations of carbonate system parameters using A_T . For example, using the r_B of Uppström (1974) rather than that of Lee et al. (2010) for evaluation of the A_T of typical surface seawater ($S = 35.0$, $t = 20.0^\circ\text{C}$, $A_T = 2350.0 \mu\text{mol kg}^{-1}$, $C_T = 2100.0 \mu\text{mol kg}^{-1}$, $P_T = 1.0 \mu\text{mol kg}^{-1}$, $S_T = 15 \mu\text{mol kg}^{-1}$) results in a difference in calculated carbonate alkalinity of about $+4.0 \mu\text{mol kg}^{-1}$.

This difference between ratios also has implications for techniques to estimate excess (i.e., organic) alkalinity from back-titrations after removal of dissolved CO_2 (e.g., Cai et al., 1998; Hernández-Ayón et al., 2007; Muller and Bleie, 2008; Yang et al., 2015). These techniques, like the one detailed here, must account for A_B in order to estimate A_X . A $4 \mu\text{mol kg}^{-1}$ difference in A_B — though small compared to seawater A_T values, which are typically in excess of $2000 \mu\text{mol kg}^{-1}$ — is remarkably significant when trying to detect excess alkalinity, which may be present in open-ocean seawater at values on the order of 4 to $8 \mu\text{mol kg}^{-1}$ (Fong and Dickson, 2019).

In general, our results highlight the need for the establishment of a “best practices” total boron to salinity ratio. The ratio of boron to chlorinity ($\text{Cl} = S/1.80655$) of 0.232 determined by Uppström (1974) is still widely used, despite the limitations in the method (Uppström, 1968) that was used to obtain it — pointed out by Liu and Lee (2009). The ratio of 0.2414 determined by Lee et al. (2010) has received recent support from measurements by Lee et al. (2019), both utilizing the same measurement technique (Liu and Lee, 2009). Ko et al. (2016) measured a

ratio of 0.2365 off the southern coast of South Korea, also using the Liu and Lee (2009) technique. Fong and Dickson (2019) suggested a ratio of 0.2354 based on the goal of increasing consistency between measured and calculated pH values in open-ocean datasets. For comparison, centering our surface GoM results at a mean value of zero excess alkalinity would require a boron to chlorinity ratio of 0.2361. A most likely universal r_B value should be established by the oceanographic community to ensure consistency and coherence in carbonate system measurements and calculations moving forward.

5. Conclusions

These results indicate a hitherto undescribed excess alkalinity component of A_T in Certified Reference Materials for oceanic CO_2 measurements. This component appears to persist despite filtration and ultraviolet treatment of CRMs, suggesting some dissolved proton acceptors may not be fully oxidized by the level of UV light applied to CRMs. Perhaps CRM preparation could benefit from enhanced irradiation, or the sourcing of seawater from a water mass with naturally low concentrations of dissolved organic proton acceptors. Either of these avenues, however, would surely be accompanied by heightened cost and/or other potential drawbacks.

Because CRMs are prepared using natural seawater, the excess alkalinity detected in this study suggests that the thermodynamic model used to describe the seawater acid–base system may be insufficient to relate A_T to other carbonate system parameters at a level of accuracy commensurate with current measurement methods. Further, excess alkalinity in CRMs may have an effect on CRM-based quality control of A_T measurements. Finally, attempts to deconvolve excess alkalinity from borate alkalinity highlight the degree of influence that the total boron to salinity ratio exerts over these investigations.

Declaration of Competing Interest

None.

Acknowledgements

Support for J.D. Sharp was provided by the National Science Foundation (NSF) Graduate Research Fellowship Program, Award #1144244, and by the William and Elsie Knight Endowed Fellowship for Marine Science from the University of South Florida College of Marine Science. This project was also supported by NSF Award #1658321. We thank Salvatore Caprara for measuring phosphate and silicate concentrations in Gulf of Mexico seawater. We are grateful also for the constructive comments of three anonymous reviewers.

Appendix A. Supplementary data

Supplementary data to this article can be found online at <https://doi.org/10.1016/j.marchem.2021.103965>.

References

- Álvarez, M., Fajar, N.M., Carter, B.C., Guallart, E.F., Pérez, F.F., Woosley, R.J., Murata, A., 2020. Global Ocean spectrophotometric pH assessment: consistent inconsistencies. *Environ. Sci. Technol.* 54, 10977–10988.
- Bockmon, E.E., Dickson, A.G., 2015. An inter-laboratory comparison assessing the quality of seawater carbon dioxide measurements. *Mar. Chem.* 171, 36–43.
- Bradshaw, A.L., Brewer, P.G., 1988. High precision measurements of alkalinity and total carbon dioxide in seawater by potentiometric titration - 1. Presence of unknown protolyte(s)? *Mar. Chem.* 23, 69–86.
- Brewer, P.G., Bradshaw, A.L., Williams, R.T., 1986. Measurements of total carbon dioxide and alkalinity in the North Atlantic Ocean in 1981. In: *The Changing Carbon Cycle*. Springer, New York, NY, pp. 348–370.
- Broek, T.A.B., Walker, B.D., Guilderson, T.P., Vaughn, J.S., Mason, H.E., McCarthy, M.D., 2020. Low molecular weight dissolved organic carbon: aging, compositional changes, and selective utilization during global ocean circulation. *Glob. Biogeochem. Cycles* 34, 1–20.

Cai, W.-J., Wang, Y., Hodson, R.E., 1998. Acid-base properties of dissolved organic matter in the estuarine waters of Georgia, USA. *Geochim. Cosmochim. Acta* 62, 473–483.

Caldeira, K., Wickett, M.E., 2003. Anthropogenic carbon and ocean pH. *Nature* 425, 365.

Carter, B.R., Radich, J.A., Doyle, H.L., Dickson, A.G., 2013. An automated system for spectrophotometric seawater pH measurements. *Limnol. Oceanogr. Methods* 11, 16–27.

Carter, B.R., Feely, R.A., Williams, N.L., Dickson, A.G., Fong, M.B., Takeshita, Y., 2018. Updated methods for global locally interpolated estimation of alkalinity, pH, and nitrate. *Limnol. Oceanogr. Methods* 16, 119–131.

Dickson, A.G., 1981. An exact definition of total alkalinity and a procedure for the estimation of alkalinity and total inorganic carbon from titration data. *Deep-Sea Res. A* 28, 609–623.

Dickson, A.G., 1990. Thermodynamics of the dissociation of boric acid in synthetic seawater from 273.15 to 318.15 K. *Deep-Sea Res. A* 37, 755–766.

Dickson, A.G., 2010. Standards for ocean measurements. *Oceanography* 23, 34–47.

Dickson, A.G., Afghan, J.D., Anderson, G.C., 2003. Reference materials for oceanic CO_2 analysis: a method for the certification of total alkalinity. *Mar. Chem.* 80, 185–197.

Dickson, A.G., Sabine, C.L., Christian, J.R. (Eds.), 2007. *Guide to Best Practices for Ocean CO_2 Measurements*, vol. 3. North Pacific Marine Science Organization, PICES Special Publication, Sidney, B.C., Canada.

Easley, R.A., Byrne, R.H., 2012. Spectrophotometric calibration of pH electrodes in seawater using purified m-cresol purple. *Environ. Sci. Technol.* 46, 5018–5024.

Ellison, S.L.R., Williams, A., 2012. Eurachem/CITAC Guide: Quantifying Uncertainty in Analytical Measurement, 3rd ed.

Feely, R.A., Sabine, C.L., Lee, K., Berelson, W., Kleypas, J., Fabry, V.J., Millero, F.J., 2004. Impact of anthropogenic CO_2 on the CaCO_3 system in the oceans. *Science* 305, 362–366.

Fong, M.B., Dickson, A.G., 2019. Insights from GO-SHIP hydrography data into the thermodynamic consistency of CO_2 system measurements in seawater. *Mar. Chem.* 211, 52–63.

Friedlingstein, P., Jones, M.W., O'Sullivan, M., Andrew, R.M., Hauck, J., Peters, G.P., Peters, W., Pongratz, J., Sitch, S., Le Quéré, C., Bakker, D.C.E., Canadell, J.G., Ciais, P., Jackson, R.B., Anthoni, P., Barbero, L., Bastos, A., Bastrikov, V., Becker, M., Bopp, L., Buitenhuis, E., Chandra, N., Chevallier, F., Chini, L.P., Currie, K.I., Feely, R.A., Gehlen, M., Gilfillan, D., Grätzalis, T., Goll, D.S., Gruber, N., Gutekunst, S., Harris, I., Haverd, V., Houghton, R.A., Hurtt, G., Ilyina, T., Jain, A.K., Joetzjer, E., Kaplan, J.O., Kato, E., Goldewijk, K.K., Korsbakken, J.I., Landschützer, P., Lauvset, S.K., Lefèvre, N., Lenton, A., Lienert, S., Lombardozzi, D., Marland, G., McGuire, P.C., Melton, J.R., Metzl, N., Munro, D.R., Nabel, J.E.M.S., Nakaoaka, S.-I., Neill, C., Omar, A.M., Ono, T., Pergon, A., Pierrot, D., Poulter, B., Rehder, G., Resplandy, L., Robertson, E., Rödenbeck, C., Séferian, R., Schwinger, J., Smith, N., Tans, P.P., Tian, H., Tilbrook, B., Tubiello, F.N., van der Werf, G.R., Wiltshire, A.J., Zeehle, S., 2019. Global carbon budget 2019. *Earth Syst. Sci. Data* 11, 1783–1838.

Hernández-Ayón, J.M., Belli, S.L., Zirino, A., 1999. pH, alkalinity and total CO_2 in coastal seawater by potentiometric titration with a difference derivative readout. *Anal. Chim. Acta* 394, 101–108.

Hernández-Ayón, J.M., Zirino, A., Dickson, A.G., Camiro-Vargas, T., Valenzuela-Espinoza, E., 2007. Estimating the contribution of organic bases from microalgae to the titration alkalinity in coastal seawaters. *Limnol. Oceanogr. Methods* 5, 225–232.

Hertkorn, N., Harir, M., Koch, B.P., Michalke, B., Schmitt-Kopplin, P., 2013. High-field NMR spectroscopy and FTICR mass spectrometry: powerful discovery tools for the molecular level characterization of marine dissolved organic matter. *Biogeosciences* 10, 1583–1624.

Holm, S., 1979. A simple sequentially rejective multiple test procedure. *Scand. J. Stat.* 6, 65–70.

Hudson-Heck, E.E., Byrne, R.H., 2019. Purification and characterization of thymol blue for spectrophotometric pH measurements in rivers, estuaries, and oceans. *Anal. Chim. Acta* 1090, 91–99.

Jones, D.L., 2017. Fathom Toolbox for MATLAB: Software for Multivariate Ecological and Oceanographic Data Analysis. College of Marine Science, University of South Florida, St. Petersburg, FL, USA. Available from: <https://www.usf.edu/marine-science/research/matlab-resources/index.aspx>.

Kim, H.C., Lee, K., 2009. Significant contribution of dissolved organic matter to seawater alkalinity. *Geophys. Res. Lett.* 36, 1–5.

King, D.W., Kester, D.R., 1989. Determination of seawater pH from 1.5 to 8.5 using colorimetric indicators. *Mar. Chem.* 26, 5–20.

Ko, Y.H., Lee, K., Eom, K.H., Han, I.S., 2016. Organic alkalinity produced by phytoplankton and its effect on the computation of ocean carbon parameters. *Limnol. Oceanogr.* 61, 1462–1471.

Lee, K., Millero, F.J., Byrne, R.H., Feely, R.A., Wanninkhof, R., 2000. The recommended dissociation constants for carbonic acid in seawater. *Geophys. Res. Lett.* 27, 229–232.

Lee, K., Kim, T.W., Byrne, R.H., Millero, F.J., Feely, R.A., Liu, Y.M., 2010. The universal ratio of boron to chlorinity for the North Pacific and North Atlantic oceans. *Geochim. Cosmochim. Acta* 74, 1801–1811.

Lee, K., Lee, C.-H., Lee, J.-H., Han, I.-S., Kim, M., 2019. Deviation of boron concentration from predictions using salinity in coastal environments. *Geophys. Res. Lett.* 46, 4809–4815.

Li, X., García-Ibáñez, M.I., Carter, B.R., Chen, B., Li, Q., Easley, R.A., Cai, W.-J., 2020. Purified meta-cresol purple dye perturbation: how it influences spectrophotometric pH measurements. *Mar. Chem.* 225, 103849.

Liu, Y.-M., Lee, K., 2009. Modifications of the curcumin method enabling precise and accurate measurement of seawater boron concentration. *Mar. Chem.* 115, 110–117.

Lueker, T.J., Dickson, A.G., Keeling, C.D., 2000. Ocean $p\text{CO}_2$ calculated from dissolved inorganic carbon, alkalinity, and equations for K_1 and K_2 : validation based on laboratory measurements of CO_2 in gas and seawater at equilibrium. *Mar. Chem.* 70, 105–119.

Mackin, J.E., 1986. The free-solution diffusion coefficient of boron: influence of dissolved organic matter. *Mar. Chem.* 20, 131–140.

McElligott, S., Byrne, R.H., 1998. Interaction of $\text{B}(\text{OH})_3$ and HCO_3^- in seawater: formation of $\text{B}(\text{OH})_2\text{CO}_3$. *Aquat. Geochem.* 3, 345–356.

McElligott, S., Byrne, R.H., Lee, K., Wanninkhof, R., Millero, F.J., Feely, R.A., 1998. Discrete water column measurements of CO_2 fugacity and pH_f in seawater: a comparison of direct measurements and thermodynamic calculations. *Mar. Chem.* 60, 63–73.

Millero, F.J., Zhang, J.Z., Lee, K., Campbell, D.M., 1993. Titration alkalinity of seawater. *Mar. Chem.* 44, 153–165.

Millero, F.J., Pierrot, D., Lee, K., Wanninkhof, R., Feely, R., Sabine, C.L., Key, R.M., Takahashi, T., 2002. Dissociation constants for carbonic acid determined from field measurements. *Deep-Sea Res. I* 49, 1705–1723.

Mojica Prieto, F.J., Millero, F.J., 2002. The values of $\text{pK}_1 + \text{pK}_2$ for the dissociation of carbonic acid in seawater. *Geochim. Cosmochim. Acta* 66, 2529–2540.

Mosley, L.M., Husheer, S.L.G., Hunter, K.A., 2004. Spectrophotometric pH measurement in estuaries using thymol blue and m-cresol purple. *Mar. Chem.* 91, 175–186.

Muller, F.L.L., Bleie, B., 2008. Estimating the organic acid contribution to coastal seawater alkalinity by potentiometric titrations in a closed cell. *Anal. Chim. Acta* 619, 183–191.

Olsen, A., Lange, N., Key, R.M., Tanhua, T., Álvarez, M., Becker, S., Bittig, H., Carter, B., Da Cunha, L.C., Van Feely, R., Heuven, S., Hoppema, M., Ishii, M., Jeansson, E., Jones, S.D., Jutterström, S., Karlsson, M.K., Kozyr, A., Lauvset, S.K., Lo Monaco, C., Murata, A., Pérez, F.F., Pfeil, B., Schirnick, C., Steinfeldt, R., Suzuki, T., Telszewski, M., Tilbrook, B., Velo, A., Wanninkhof, R., 2019. GLODAPv2.2019: an update of GLODAPv2. *Earth Syst. Sci. Data* 11, 1437–1461.

Orr, J.C., Fabry, V.J., Aumont, O., Bopp, L., Doney, S.C., Feely, R.A., Gnanadesikan, A., Gruber, N., Ishida, A., Joos, F., Key, R.M., Lindsay, K., Maier-Reimer, E., Matear, R., Monfray, P., Mouchet, A., Najjar, R.G., Plattner, G.K., Rodgers, K.B., Sabine, C.L., Sarmiento, J.L., Schiltz, R., Slater, R.D., Totterdell, I.J., Weirig, M.F., Yamanaka, Y., Yool, A., 2005. Anthropogenic Ocean acidification over the twenty-first century and its impact on calcifying organisms. *Nature* 437, 681–686.

Orr, J.C., Epitalon, J.-M., Dickson, A.G., Gattuso, J.-P., 2018. Routine uncertainty propagation for the marine carbon dioxide system. *Mar. Chem.* 207, 84–107.

Parsons, T.R., 1984. *A Manual of Chemical & Biological Methods for Seawater Analysis*. Pergamon Press.

Patsavas, M.C., Byrne, R.H., Wanninkhof, R., Feely, R.A., Cai, W.J., 2015. Internal consistency of marine carbonate system measurements and assessments of aragonite saturation state: insights from two U.S. coastal cruises. *Mar. Chem.* 176, 9–20.

Sharp, J.D., Byrne, R.H., 2020. Interpreting measurements of total alkalinity in marine and estuarine waters in the presence of proton-binding organic matter. *Deep-Sea Res. Part I* 165, 103338.

Sharp, J.D., Pierrot, D., Humphreys, M.P., Epitalon, J.-M., Orr, J.C., Lewis, E.R., Wallace, D.W.R., 2020. CO2SYSv3 for MATLAB (version 3.1). Zenodo. <https://doi.org/10.5281/zenodo.4023039>.

Sipos, P., May, P.M., Hefer, G.T., 2000. Carbonate removal from concentrated hydroxide solutions. *Analyst* 125, 955–958.

Uppström, L.R., 1968. A modified method for determination of boron with curcumin and a simplified water elimination procedure. *Anal. Chim. Acta* 43, 475–486.

Uppström, L.R., 1974. The boron/chlorinity ratio of deep-sea water from the Pacific Ocean. *Deep-Sea Res.* 21, 161–162.

Williams, N.L., Juranek, L.W., Feely, R.A., Johnson, K.S., Sarmiento, J.L., Talley, L.D., Dickson, A.G., Gray, A.R., Wanninkhof, R., Russell, J.L., Riser, S.C., Takeshita, Y., 2017. Calculating surface ocean $p\text{CO}_2$ from biogeochemical Argo floats equipped with pH: an uncertainty analysis. *Glob. Biogeochem. Cycles* 31, 591–604.

Wolf-Gladrow, D.A., Zeebe, R.E., Klaas, C., Körtzinger, A., Dickson, A.G., 2007. Total alkalinity: the explicit conservative expression and its application to biogeochemical processes. *Mar. Chem.* 106, 287–300.

Woosley, R.J., 2021. Evaluation of the Temperature Dependence of Dissociation Constants for the Marine Carbon System Using pH and Certified Reference Materials. *Mar. Chem.* 229, 103914.

Yang, B., Byrne, R.H., Lindemuth, M., 2015. Contributions of organic alkalinity to total alkalinity in coastal waters: a spectrophotometric approach. *Mar. Chem.* 176, 199–207.

Yao, W., Byrne, R.H., 1998. Simplified seawater alkalinity analysis: Use of linear array spectrometers. *Deep-Sea Res. Part I* 45, 1383–1392.

Zhang, H., Byrne, R.H., 1996. Spectrophotometric pH measurements of surface seawater at in-situ conditions: absorbance and protonation behavior of thymol blue. *Mar. Chem.* 52, 17–25.